and a fourth partition comprising skull, fat, muscle and voxels which have a high degree of partial voluming and thus cannot be included in one of the other three groups. The image sets were smoothed with an isotropic Gaussian filter (12 mm FWHM), and individual global counts were normalised by proportional scaling to a mean value of 5.0.

Determination of regional metabolic reduction and grey matter loss ROI maps in AD

First, normalised PET and grey matter MRI data sets of 30 healthy volunteers in the first group and the mild AD group were compared on a voxel-by-voxel basis using a two-sample *t* test in SPM99. Significance was accepted if the voxels survived a corrected threshold of $p<0.01$. Then we defined ROI maps for PET and segmented MRI obtained from the comparison of the mild AD group and the first healthy group.

Next, prediction of AD was evaluated in very mild AD patients and the other 30 healthy volunteers in the second group using free software, the easy Z score Imaging System (eZIS) (Daiichi Radioisotope Laboratory, Tokyo, Japan); the concept of eZIS is the same as the concept of the system described in a previous study [21]. *Z* scores were calculated for each PET and segmented MR image in the very mild AD patients and the second group of healthy volunteers by comparison with the mean and SD of PET and segmented MR images in the first group of healthy volunteers. *Z* score was calculated as: *Z* score=[(normal mean)−(individual value)]/(normal SD).

We performed a receiver operating characteristic (ROC) analysis with maximum *Z* scores in the ROIs. The maximum *Z* score was automatically extracted from all of the *Z* scores of the ROI maps in the very mild AD group and the second healthy group using additional software implemented on MATLAB (Mathworks Inc., MA, USA). ROC analysis was performed using the maximum *Z* score and ROCKIT software 0.9B (Dr. Metz, Department of Radiology, The University of Chicago, IL, USA). The areas under the curves and accuracy were calculated. Additionally, combined (summed) maximum *Z* scores of individual PET and segmented MR images in the very mild AD group and the second group of healthy volunteers were calculated and ROC analysis was performed.

Results

ROI maps

In the FDG-PET study, metabolic reduction was demonstrated in the bilateral posterior cingulate gyri and the right parietotemporal area in the mild AD group as compared with the first healthy control group ($p<0.01$, corrected) (Fig. 1, Table 1).

In the MRI-VBM study, the grey matter density of the amygdala and hippocampal complex and the bilateral temporal and frontal gyri in the mild AD group was significantly lower than that in the first healthy control group ($p<0.01$, corrected) (Fig. 2, Table 2).

Based on these results, ROI maps for PET and MRI were produced (Fig. 3).

ROC analysis and the diagnostic value of very mild AD with FDG-PET and VBM-MRI

Figure 4 shows the ROC curves for FDG-PET, VBM-MRI and the combination of FDG-PET and VBM-MRI. The accuracy of FDG-PET diagnosis was 88.5%, and that of VBM-MRI, 82.9%. The area under the ROC curve for FDG-PET was 0.953 and that for VBM-MRI, 0.910.

The area under the ROC curve and the diagnostic accuracy of FDG-PET were higher than those of VBM-MRI; however, there was no significant difference in the partial area index for ROC curves between FDG-PET and VBM-MRI ($p=0.435$). The area under the ROC curve and the diagnostic accuracy of the combination of FDG-PET and VBM-MRI were 0.985 and 93.5%.

Representative cases

Figure 5 shows the *Z* score maps of a 67-year-old female with very mild AD. The FDG-PET *Z* score map

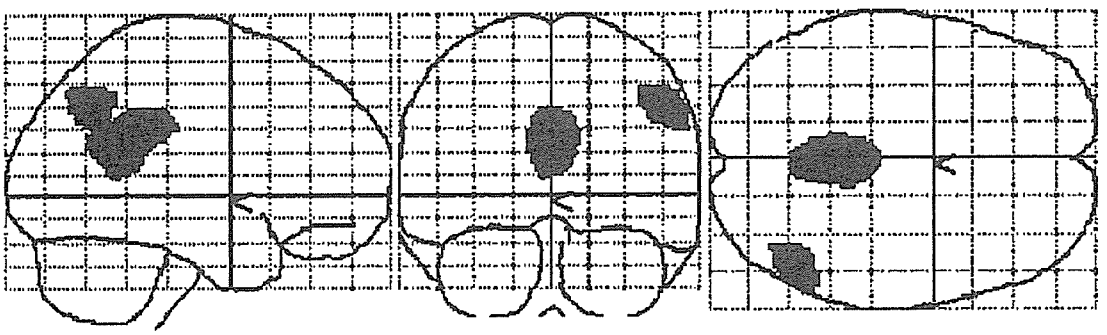

Fig. 1. Statistical parametric mapping (SPM) projections showing areas with significantly reduced glucose metabolism ($p<0.01$, corrected) in a comparison of 30 patients with mild AD and 30 normal control subjects (first group)

Table 1. Peak location of significant metabolic reduction in the mild AD group as compared with the NC group ($p<0.01$, corrected)

	t value	*x*	*y*	*z*
Cingulate gyrus	6.74	0	−33	33
Rt. angular gyrus	6.08	57	−57	34
Lt. precuneus	5.25	−36	−68	42
Rt. inferior temporal gyrus	5.24	65	−38	−18
Lt. inferior temporal gyrus	5.20	−63	−40	−18
Lt. middle temporal gyrus	5.10	−67	−32	−10

Coordinates are in millimetres, relative to the anterior commissure, corresponding to the atlas of Talairach and Tournoux

x, distance (mm) to right (−) or left (+) of the midsagittal line; *y*, distance anterior (+) or posterior (−) to vertical plane through the anterior commissure; *z*, distance above (+) or below (−) the intercommissural line

demonstrates significant metabolic reduction in the bilateral posterior cingulate gyri, parietal association cortices and frontal association cortices. The maximum *Z* score of the ROI was 4.01. The VBM-MRI *Z* score map shows significant grey matter loss in the bilateral medial and lateral temporal lobes and a mild decrease in the left occipital lobe. The maximum *Z* score of the ROI was 4.08.

Figure 6 shows *Z* score maps of a 72-year-old female healthy volunteer. There is no significant metabolic reduction or grey matter loss, though frontal base metabolism and temporal grey matter are slightly decreased.

Discussion

We performed FDG-PET and MRI in the same individual subjects with very mild AD and compared the diagnostic accuracy of the two modalities using ROC analysis. The application of SPM and VBM to the atrophied brain and diagnosis is still controversial [22, 23]. However, we employed a combination of structural images and statistical *Z* score images to obtain a clinical diagnosis of mild AD. For practical clinical purposes, such a combination allows accurate diagnosis of AD [12]. Though there is no perfect way to evaluate and compare directly the diagnostic accuracy of FDG-PET and MRI, we consider that ours is an objective method for this purpose. This type of study design should be tested in assessing diagnostic performance in future studies.

The medial temporal area is pathologically affected even in the early stages of AD. Using MRI, medial temporal volume loss has been shown in previous reports [24–30], and the present study substantiated this finding in mild AD patients. Even in subjects with mild cognitive impairment, the VBM method has been found to demonstrate a significant reduction in grey matter density [31]. As regards medial temporal glucose metabolism, the value of estimating hippocampal metabolism has not been recognised although recently Mosconi et al. reported reduced hippocampal metabolism in patients with mild cognitive impairment and AD using their new automated analysis technique [32]. Our study did not demonstrate hippocampal glucose hypometabolism in early AD, in agreement with previous reports [5, 33]. We assume this was due to the use of a voxel-based comparison technique, as Mosconi et al. also failed to demonstrate hippocampal hypometabolism when they used a voxel-based comparison technique. The utility of demonstrating hippocampal hypometabolism in early AD should be re-examined if the technique of Mosconi et al. becomes available in other institutes.

Reduced metabolism and perfusion in the posterior cingulate gyrus in AD have been well recognised by previous studies using PET [34, 35] and SPECT [36]. Our study verified this pathophysiology in mild AD patients. There are also well-documented strong reciprocal connections between the hippocampus and the temporoparietal association cortex, showing that neuronal damage in the hippocampus, which occurs at an early stage of AD, may impair the synaptic function in the associated neocortex. However, histopathological involvement of the posterior cingulate gyrus in AD is not as severe as involvement of the medial temporal lobes at a mild stage of the disease.

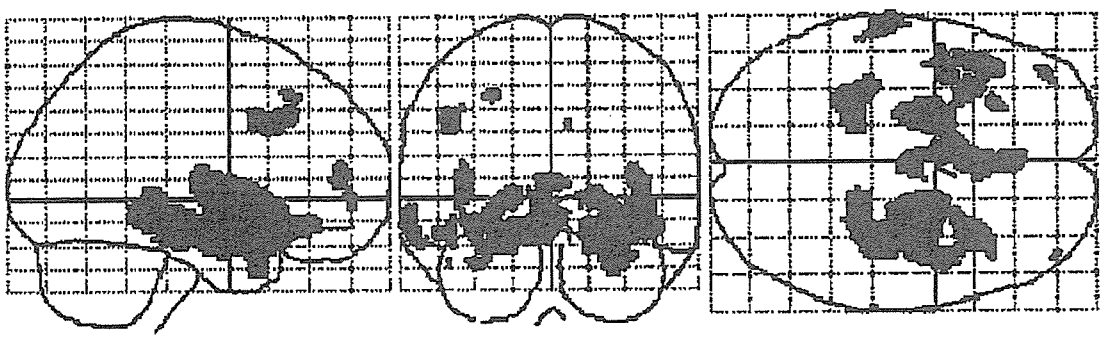

Fig. 2. SPM projections showing areas with significantly reduced grey matter density ($p<0.01$, corrected) in the comparison of mild AD patients and normal control subjects (first group). Grey matter density in the bilateral medial temporal lobe, including the amygdala, hippocampus and parahippocampal gyrus, in the mild AD group was significantly lower than that in the normal control group

Table 2. Peak location of significant reduction in cortical density in the mild AD group compared with the NC group ($p< 0.01$, corrected)

	t value	*x*	*y*	*z*
Rt. parahippocampal gyrus	8.88	26	−6	−13
Lt. anterior cingulate	7.67	−2	17	−9
Lt. middle temporal gyrus	6.80	−63	−22	−9
Lt. hippocampus	6.54	−26	−35	0
Lt. middle frontal gyrus	6.43	−44	17	30
Lt. insula	6.04	−38	8	1
Lt. middle frontal gyrus	5.93	−40	49	5
Lt. middle frontal gyrus	5.89	−26	29	41
Rt. middle frontal gyrus	5.75	42	52	−1
Lt. middle temporal gyrus	5.67	−55	−32	−14
Lt. superior temporal gyrus	5.67	−48	3	−14
Rt. cingulate gyrus	5.52	8	19	30
Rt. middle temporal gyrus	5.50	65	−26	−12
Lt. superior temporal gyrus	5.50	−46	14	−26

Coordinates are in millimetres, relative to the anterior commissure, corresponding to the atlas of Talairach and Tournoux
x, distance (mm) to right (−) or left (+) of the midsagittal line; *y*, distance anterior (+) or posterior (−) to vertical plane through the anterior commissure; *z*, distance above (+) or below (−) the intercommissural line

This neuronal connection from the pathologically affected medial temporal structures may explain the metabolic reduction in the posterior cingulate gyrus, especially at an early stage of AD. Even if the synaptic dysfunction in the posterior cingulate gyrus is based on the secondary pathological effect in medial temporal structures, our results suggest that FDG-PET is more reliable than MRI in diagnosing very early AD. This may be due to the anatomical variance in normal subjects, which increases the standard deviation of grey matter distribution and decreases the accuracy of MRI in discriminating AD from normal findings.

Our study also verified previous findings that the application of *Z* score maps by voxel-based comparison with a normal data set improves diagnostic accuracy [21, 33]. Kanetaka et al. [37] used the same data analysis technique as was employed in the present study to assess the accuracy of ECD-SPECT for the diagnosis of very mild AD. Their subjects were 61 patients with very mild AD (mean age 70.6 years, mean MMSE score 26.0), and the authors showed an accuracy of 83.9%, with the area under the ROC curve measuring 0.906. Although direct comparison of their study and our own is not possible, we hypothesise that FDG-PET offers a better diagnostic performance for very mild AD.

Although FDG-PET has a higher accuracy for the clinical diagnosis of AD, MRI remains a necessary tool to exclude other conditions such as infarction and subdural haematoma. If three-dimensional MRI techniques like SPGR imaging are used, the images can be analysed with VBM, and *Z* score images can be produced. As shown in our study, the diagnostic performance of MRI demonstrated as a *Z* score map can improve accuracy, and routine clinical three-dimensional MRI may be the first choice for the diagnosis of mild AD. The diagnostic performance of MRI was nearly as good as that of FDG-PET when a VBM-MRI *Z* score map was produced. However, it must not be forgotten that the value of FDG-PET in the management of AD patients extends beyond diagnosis, e.g. it offers information on the cortical metabolic status and permits differential diagnosis of other degenerative dementias [38, 39]. FDG-PET documents not only parietotemporal and posterior cingulate metabolic impairment but also metabolic impairment in frontal or other regions that manifests as depression or other disorders [40–42]. Clinically, FDG-PET is recommended for early intervention with medication for AD. Further studies focussing on the cost-effectiveness of FDG-PET are needed to evaluate its role in the diagnosis of very early AD.

In conclusion, we demonstrated high accuracy of both FDG-PET and VBM-MRI with *Z* score mapping in diagnosing the very early stages of AD and showed that FDG-PET has a relatively higher accuracy than MRI. However, as the additional evaluation showed, combina-

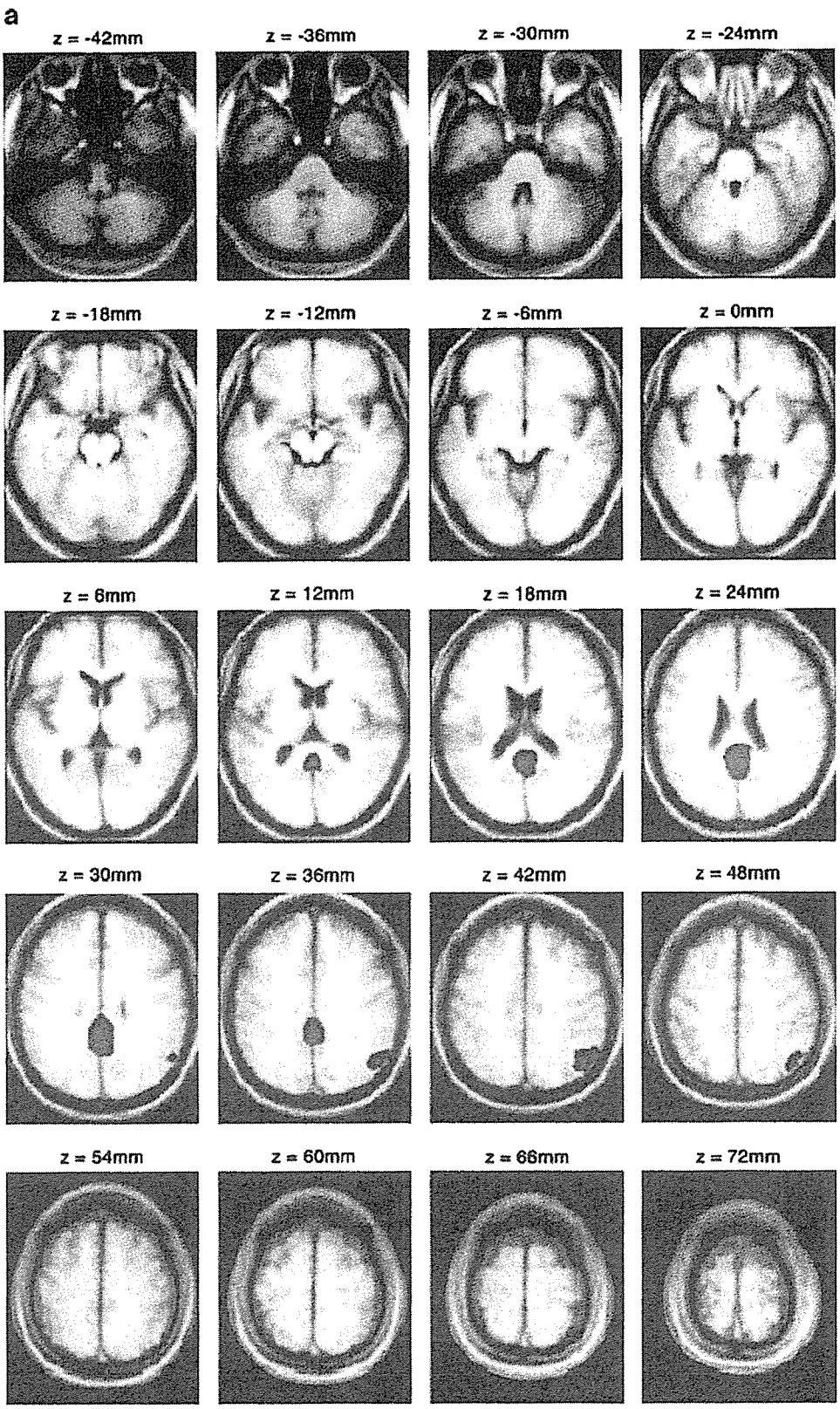

Fig. 3. ROI maps for PET (**a**) and MRI (**b**) which were obtained from the analysis in the mild AD group and the first normal group

Fig. 3. (continued)

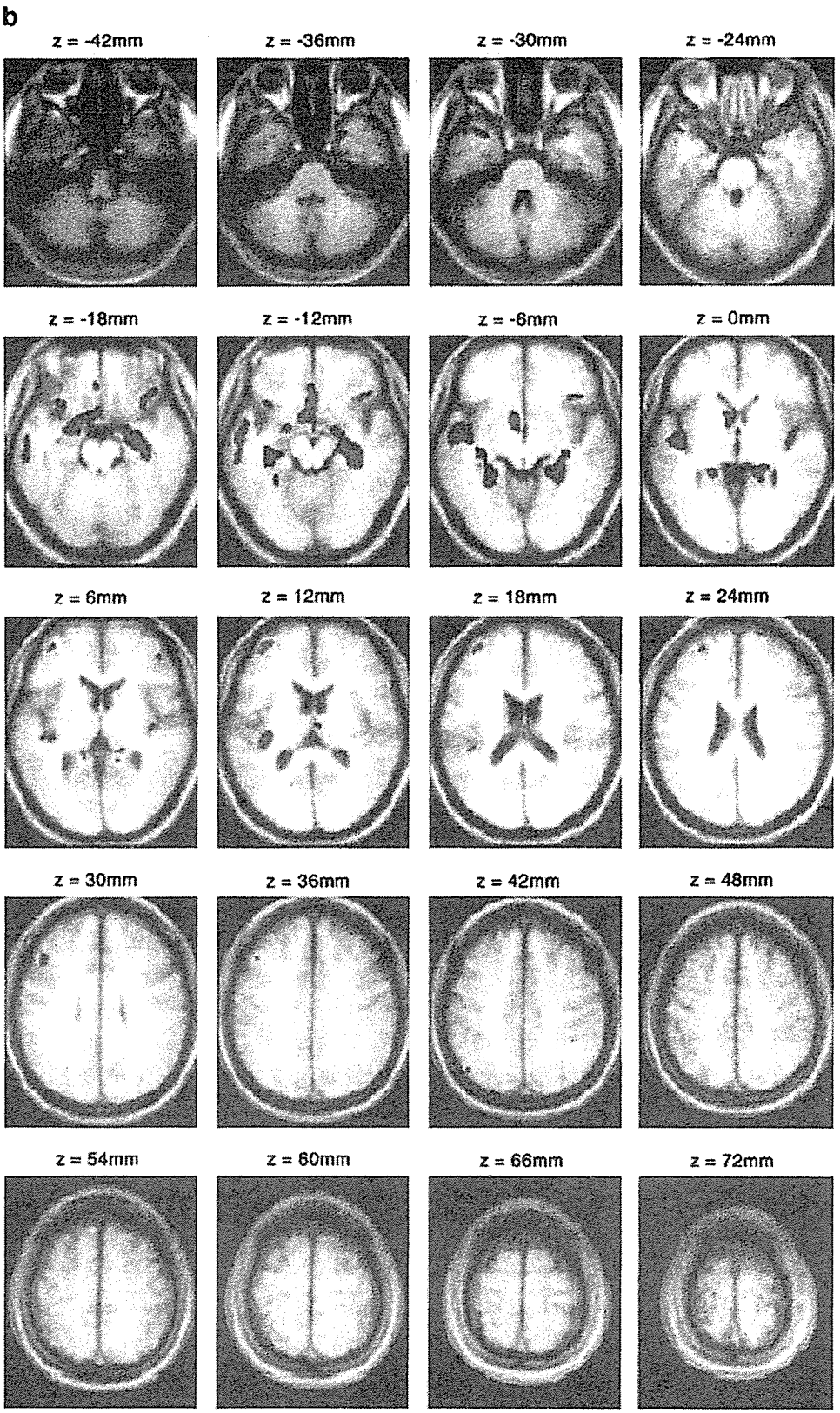

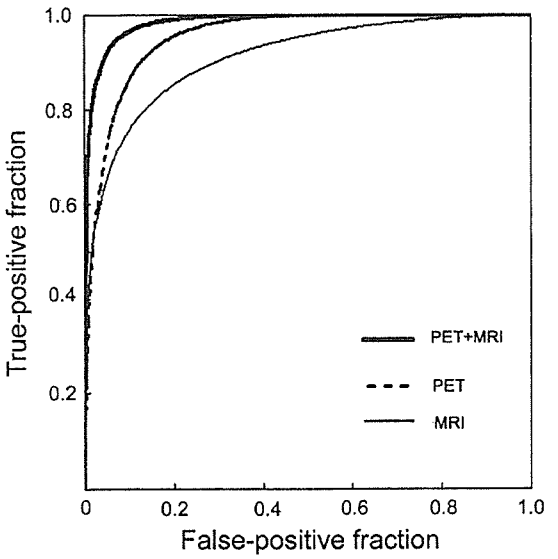

Fig. 4. ROC curves for PET and MRI diagnostic performances. The area under the ROC curve for PET (A_z=0.953) was slightly larger than that for MRI (A_z=0.910). The area under the ROC curve for the combination of PET and MRI was the largest (A_z=0.985). True-positive fraction=sensitivity; false-positive fraction=1−specificity

tion of the two techniques improved the diagnostic performance. When using only one method, FDG-PET is better than VBM-MRI for detecting very mild AD, but

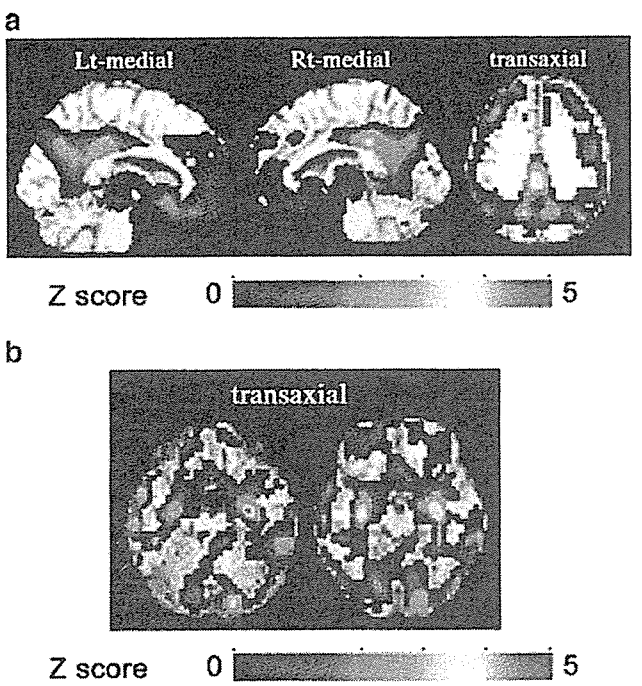

Fig. 5. *Z* score maps of a 67-year-old female with very mild AD (MMSE score=26). **a** *Z* score map of FDG-PET. **b** *Z* score map of VBM-MRI

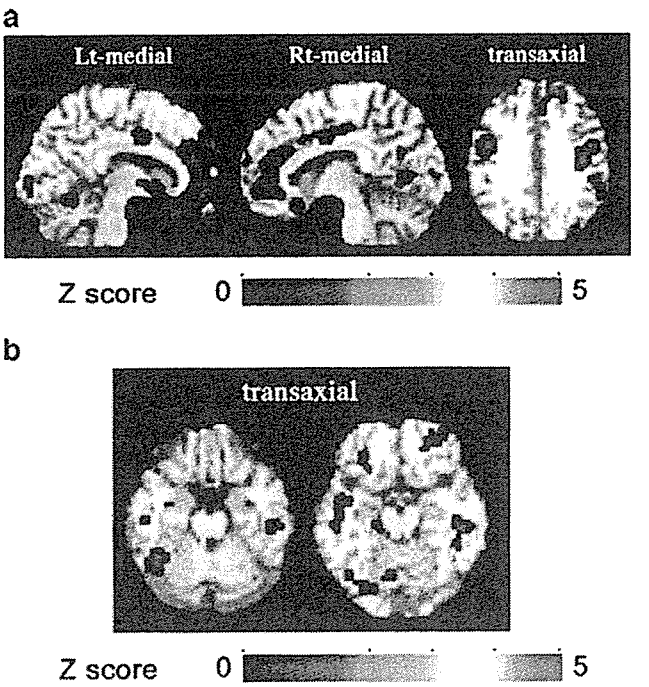

Fig. 6. *Z* score map of one healthy volunteer (72-year-old female). **a** *Z* score map of FDG-PET. The maximum *Z* score of the ROI was 0.60. **b** *Z* score map of VBM-MRI. The maximum *Z* score of the ROI was 2.48. There is no significant metabolic reduction and no area with a significant decrease in grey matter density

when both methods are available, a combination of FDG-PET and MRI-VBM should be performed.

References

1. Grundman M, Sencakova D, Jack CR Jr, Petersen RC, Kim HT, Schultz A, et al. Alzheimer's Disease Cooperative Study. Brain MRI hippocampal volume and prediction of clinical status in a mild cognitive impairment trial. J Mol Neurosci 2002;19:23–27
2. Karas GB, Scheltens P, Rombouts SA, Visser PJ, van Schijndel RA, Fox NC, et al. Global and local gray matter loss in mild cognitive impairment and Alzheimer's disease. Neuroimage 2004;23:708–716
3. de Leon MJ, DeSanti S, Zinkowski R, Mehta PD, Pratico D, Segal S, et al. MRI and CSF studies in the early diagnosis of Alzheimer's disease. J Intern Med 2004;256:205–223
4. de Toledo-Morrell L, Stoub TR, Bulgakova M, Wilson RS, Bennett DA, Leurgans S, et al. MRI-derived entorhinal volume is a good predictor of conversion from MCI to AD. Neurobiol Aging 2004;25:1197–1203
5. Minoshima S, Giordani B, Berent S, Frey KA, Foster NL, Kuhl DE. Metabolic reduction in the posterior cingulate cortex in very early Alzheimer's disease. Ann Neurol 1997;42:85–94
6. Mosconi L. Brain glucose metabolism in the early and specific diagnosis of Alzheimer's disease. FDG-PET studies in MCI and AD. Eur J Nucl Med Mol Imaging 2005;32:486–510
7. Mosconi L, Perani D, Sorbi S, Herholz K, Nacmias B, Holthoff V, et al. MCI conversion to dementia and the APOE genotype: a prediction study with FDG-PET. Neurology 2004; 63:2332–2340

8. Herholz K. PET studies in dementia.Ann Nucl Med 2003;17:79–89
9. Ashburner J, Friston KJ. Voxel-based morphometry—the methods. Neuroimage 2000;11:805–821
10. Baron JC, Chetelat G, Desgranges B, Perchey G, Landeau B, de la Sayette V, et al. In vivo mapping of gray matter loss with voxel-based morphometry in mild Alzheimer's disease. Neuroimage 2001;14:298–309
11. Burton EJ, Karas G, Paling SM, Barber R, Williams ED, Ballard CG, et al. Patterns of cerebral atrophy in dementia with Lewy bodies using voxel-based morphometry. Neuroimage 2002;17:618–630
12. Ishii K, Kawachi T, Sasaki H, Kono AK, Fukuda T, Kojima Y, et al. Voxel-based morphometric comparison between early- and late-onset mild Alzheimer's disease and assessment of diagnostic performance of Z score images. AJNR Am J Neuroradiol 2005;25:333–340
13. Ishii K, Sasaki H, Kono AK, Miyamoto N, Fukuda T, Mori E. Comparison of gray matter and metabolic reduction in mild Alzheimer's disease using FDG-PET and voxel-based morphometric MR studies. Eur J Nucl Med Mol Imaging 2005; 32:959–963
14. McKhann G, Drachman D, Folstein M, Katzman R, Price D, Stadlan EM. Clinical diagnosis of Alzheimer's disease: report of the NINCDS-ADRDA Work Group under the auspices of Department of Health and Human Services Task Force on Alzheimer's disease. Neurology 1984;34:939–944
15. Folstein MF, Folstein SE, McHugh PR. "Mini-mental state". A practical method for grading the cognitive state of patients for the clinician. J Psychiat Res 1975;12:189–198
16. Honma A, Fukuzawa K, Tsukada Y, Ishii T, Hasegawa K, Mohs RC. Development of a Japanese version of Alzheimer's Disease Assessment Scale (ADAS). Jpn J Geriatr Psychiatry 1992; 647–655
17. Ishii K, Sasaki M, Kitagaki H, Yamaji S, Sakamoto S, Matsuda K, et al. Reduction of cerebellar glucose metabolism in advanced Alzheimer's disease. J Nucl Med 1997;38:925–928
18. Friston KJ, Ashburner J, Frith CD, Poline J-B, Heather JD, Frackowiak RSJ. Spatial registration and normalization of images. Human Brain Mapping 1995;3:165–189
19. Ashburner J, Neelin P, Collins DL, Evans AC, Friston KJ. Incorporating prior knowledge into image registration. Neuroimage 1997;6:344–352
20. Ashburner J, Friston KJ. Nonlinear spatial normalization using basis functions. Human Brain Mapping 1999;7:254–266
21. Ishii K, Sasaki M, Matsui M, Sakamoto S, Yamaji S, Hayashi N, et al. A diagnostic method for suspected Alzheimer's disease using $H_2{}^{15}O$ positron emission tomography perfusion Z score. Neuroradiology 2000;42:787–794
22. Bookstein FL. "Voxel-based morphometry" should not be used with imperfectly registered images. Neuroimage 2001; 14:1454–1462
23. Ashburner J, Friston KJ. Why voxel-based morphometry should be used. Neuroimage 2001;14:1238–1243
24. Kesslak JP, Nalcioglu O, Cotman CW. Quantification of magnetic resonance scans for hippocampal atrophy in Alzheimer's disease. Neurology 1991;41:51–54
25. Scheltens P, Leys D, Barkhof F, Huglo D, Weinstein HC, Vermersch P, et al. Atrophy of medial temporal lobes on MRI in "probable" Alzheimer's disease and normal ageing: diagnostic value and neuropsychological correlates. J Neurol Neurosurg Psychiatry 1992;55:967–972
26. Jack CR, Petersen RC, O'Brien PC, Tangalos EG. MR-based hippocampal volumetry in the diagnosis of Alzheimer's disease. Neurology 1992;42:183–188
27. Watson C, Andermann F, Gloor P, Jones-Gotman M, Peters T, Evans A, et al. Anatomic basis of amygdaloid and hippocampal volume measurement by magnetic resonance imaging. Neurology 1992;42:1743–1750
28. de Leon MJ, Golomb J, George AE, Convit A, Tarshish CY, McRae T, et al. The radiologic prediction of Alzheimer's disease: the atrophic hippocampal formation. AJNR 1993;14:897–906
29. Kiliany RJ, Moss MB, Albert MS, Sandor T, Tieman J, Jolesz F. Temporal lobe regions on magnetic resonance imaging identify patients with early Alzheimer's disease. Arch Neurol 1993;50:949–954
30. Lehéricy S, Baulac M, Chiras J, Pierot L, Martin N, Pillon B, et al. Amygdalohippocampal MR volume measurements in the early stages of Alzheimer's disease. AJNR 1994;15:927–937
31. Chetelat G, Desgranges B, De La Sayette V, Viader F, Eustache F, Baron JC. Mapping gray matter loss with voxel-based morphometry in mild cognitive impairment. Neuroreport 2002;13:1939–19343
32. Mosconi L, Tsui WH, De Santi S, Li J, Rusinek H, Convit A, et al. Reduced hippocampal metabolism in MCI and AD: automated FDG-PET image analysis. Neurology 2005;64:1860–1867
33. Burdette JH, Minoshima S, Vander Borght T, Tran DD, Kuhl DE. Alzheimer disease: improved visual interpretation of PET images by using three-dimensional stereotaxic surface projections. Radiology 1996;198:837–843
34. Ishii K, Sasaki M, Yamaji S, Sakamoto S, Kitagaki H, Mori E. Demonstration of decreased posterior cingulate perfusion in mild Alzheimer's disease by means of $H_2{}^{15}O$ positron emission tomography. Eur J Nucl Med 1997;24:670–673
35. Ishii K. Clinical application of positron emission tomography for diagnosis of dementia. Ann Nucl Med 2002;16:515–525
36. Bartenstein P, Minoshima S, Hirsch C, Buch K, Willoch F, Mosch D, et al. Quantitative assessment of cerebral blood flow in patients with Alzheimer's disease by SPECT. J Nucl Med 1997;38:1095–1101
37. Kanetaka H, Matsuda H, Asada T, Ohnishi T, Yamashita F, Imabayashi E, et al. Effects of partial volume correction on discrimination between very early Alzheimer's dementia and controls using brain perfusion SPECT. Eur J Nucl Med Mol Imaging 2004;31:975–980
38. Ishii K, Sakamoto S, Sasaki M, Kitagaki H, Yamaji S, Hashimoto M, et al. Cerebral glucose metabolism in patients with frontotemporal dementia. J Nucl Med 1998;39:1875–1878
39. Ishii K, Imamura T, Sasaki M, Yamaji S, Sakamoto S, Kitagaki H, et al. Regional cerebral glucose metabolism in dementia with Lewy bodies and Alzheimer's disease. Neurology 1998;51:125–130
40. Hirono N, Mori E, Ishii K, Ikejiri Y, Imamura T, Shimomura T, et al. Frontal lobe hypometabolism and depression in Alzheimer's disease. Neurology 1998;50:380–383
41. Hirono N, Mori E, Ishii K, Ikejiri Y, Imamura T, Shimomura T, et al. Regional hypometabolism related to language disturbance in Alzheimer's disease. Dement Geriatr Cogn Disord 1998;9:68–73
42. Hirono N, Mori E, Ishii K, Kitagaki H, Sasaki M, Ikejiri Y, et al. Alteration of regional cerebral glucose utilization with delusions in Alzheimer's disease. J Neuropsychiat Clin Neurosci 1998;10:433–439

ELSEVIER

NeuroImage

www.elsevier.com/locate/ynimg
NeuroImage 32 (2006) 301 – 306

Relationship between antisocial behavior and regional cerebral blood flow in frontotemporal dementia

Seigo Nakano,[a,b,*] Takashi Asada,[c] Fumio Yamashita,[d] Noriko Kitamura,[e] Hiroshi Matsuda,[f] Shigeo Hirai,[g] and Tatsuo Yamada[a]

[a]*Fifth Department of Internal Medicine, School of Medicine, Fukuoka University, Japan*
[b]*Department of Geriatric Medicine, National Center Hospital for Mental, Nervous, and Muscular Disorders, National Center of Neurology and Psychiatry (NCNP), Japan*
[c]*Department of Psychiatry, School of Medicine, Tsukuba University, Japan*
[d]*National Institute of Neuroscience, National Center of Neurology and Psychiatry (NCNP), Japan*
[e]*Department of Psychiatry, Tokyo Metropolitan Fuchyu Hospital, Japan*
[f]*Department of Nuclear Medicine, Saitama Medical School Hospital, Japan*
[g]*Department of Psychiatry, National Center Hospital for Mental, Nervous, and Muscular Disorders, National Center of Neurology and Psychiatry (NCNP), Japan*

Received 28 November 2005; revised 10 February 2006; accepted 28 February 2006
Available online 19 April 2006

Objective: **To examine the relationship between antisocial behaviors and reduction of regional cerebral blood flow (rCBF) in patients with frontotemporal dementia (FTD).**

Methods: **Brain perfusion single photon emission computed tomography (SPECT) was performed in 22 patients with FTD and 76 age-matched healthy volunteers. The statistical analysis was conducted using the SPM99 software. The antisocial behavioral symptoms were assessed independently by three geriatric psychiatrists, who had not been given the information of the SPECT images.**

Results: **Compared with normal controls, FTD patients showed significant reduction of rCBF in the widespread frontal cortical areas. The correlation analysis showed that antisocial behavioral symptoms are associated with reduction of rCBF in the orbitofrontal cortex.**

Conclusion: **The functional decline of orbitofrontal cortex is related to antisocial behavioral symptoms in patients with FTD.**

Keywords: Frontotempotal dementia; Antisocial behaviors; SPECT; Regional cerebral blood flow

Introduction

Frontotemporal lobar degeneration (FTLD) is composed of a spectrum of dementing disorders with degeneration of the frontal lobes, the anterior temporal lobes, or the both (Neary et al., 1998). Frontotemporal dementia (FTD) is the main FTLD syndrome and manifests as prominent personality and behavioral disturbances. Behavioral symptoms such as antisocial behaviors are observed in patients with FTD, and presence of them often makes it difficult to care for such patients. Moreover, such symptoms will prompt their institutionalization. Development of appropriate management methods for the behavioral symptoms may lessen the care-giving burden and lead to postponement of institutionalization. Evaluation of antisocial behavioral symptoms in FTD patients must be the basis for such development.

Systematic functional neuroimaging studies using single photon emission computed tomography (SPECT) or positron computed tomography (PET) have demonstrated that patients with FTD show hypoperfusion of anterior cerebral cortex with relative sparing of posterior cortex (Ishii et al., 1998; Miller and Gearhart, 1999; Charpentier et al., 2000; Hodges, 2001; Lojkowska et al., 2002). These evidences have become useful to make clinical diagnosis of FTD. However, systemic studies examining the association between antisocial behavior and regional cerebral blood flow (rCBF) in patients with FTD are few and mostly based on visual inspection (Mychack et al., 2001) using the region of interest (ROI) method. Although this approach has been popular, accuracy depends on the observer's experience and working-hypothesis, thus such evaluation is apt to lack morphological accuracy of brain regions and leaves large areas of the brain unexplored. An alternative method is voxel-by-voxel analysis of stereotactic space, which adopts the principle of data-driven analysis and can avoid subjectivity. Such an approach is well established in the field of functional neuroimaging analysis; a software package known as statistical parametric mapping (SPM), that not only spatially normalizes PET or SPECT images to a standardized stereotactic space but also statistically analyzes group of images, has been

* Corresponding author. Fifth Department of Internal Medicine, Fukuoka University, Japan. Fax: +81 92 865 7900.
E-mail address: scigo-n@fukuoka-u.ac.jp (S. Nakano).
Available online on ScienceDirect (www.sciencedirect.com).

1053-8119/$ - see front matter © 2006 Elsevier Inc. All rights reserved.
doi:10.1016/j.neuroimage.2006.02.040

developed (Frackowiack et al., 1997). The objective of this study is to evaluate the relationship between antisocial behavior and rCBF abnormalities in FTD patients by application of SPM to brain perfusion SPECT images.

Materials and methods

Subjects

Twenty-two consecutive patients (14 men, 8 women; age range, 58–74 years; mean age, 62.9 years) newly referred to the memory disorder clinic of the National Center Hospital for Mental, Nervous, and Muscular Disorders, National Center of Neurology and Psychiatry, Tokyo, Japan, between 1994 and 2003, were enrolled. The mean age at onset was 57.5 years (range, 47–68 years). The clinical diagnosis of FTD was based on the Lund and Manchester criteria and the more recent consensus criteria (Neary et al., 1998) after detailed examination, including magnetic resonance imaging (MRI), SPECT, and neuropsychological examination. The clinical criteria of FTD are reported to have high diagnostic specificities (Rosen et al., 2002). The neuropsychological battery consisted of tests that have been shown to be useful in the differential diagnosis of FTD and other dementia. The following tests were employed: Mini Mental State Examination (MMSE) (Folstein et al., 1975), Revised Version of Hasegawa's Dementia Scale (HDS-R) (Imai and Hasegawa, 1999), Raven's Colored Progressive Matrices (RCPM) (Hodges, 1993), Digit Span Task, learning of a list of 10 words and Story Recall (Hodges, 1993), Ray-Osterrieth Complex Figure Test (Hodges, 1993), Stroop Test, and Trail Making Test (Anne and Stephan, 1969). All tests were performed and scored according to the standard protocols. The demographic characteristics of the patients including age, sex, MMSE, and HDS-R at the time of the first evaluation are listed in Table 1.

Seventy-six normal healthy volunteers (37 men, 39 women; age range, 67–87 years; mean age ± SD, 71.0 ± 7.1 years) were also studied. They had no neurologic or psychiatric disorders, including alcoholism, substance abuse, atypical headache, head trauma with loss of consciousness, and asymptomatic cerebral infarction detected by T2-weighted MRI. They did not significantly differ in age, sex, or education from the FTD patients.

SPECT image data of the normal healthy volunteers in the present study have previously been reported (Imabayashi et al., 2004).

Written informed consent was obtained from all the participants or their family according to the Declaration of Helsinki. The study was approved by the Ethical Committee of the National Center of Neurology and Psychiatry.

Assessment of antisocial behaviors

Semi-structured interviews with the family members were conducted to obtain information regarding the behaviors of interest. For the interview, we used the modified version of Neuropsychiatric Inventory (NPI) (Cummings et al., 1994). By applying the method of NPI, which assesses the Behavioral and Psychological Symptoms of Dementia (BPSD) in patients basically with Alzheimer's disease, the antisocial behaviors were evaluated as follows. The frequency and severity were respectively graded for the 5 behavioral symptoms based on the study by Miller et al. (1997): (1) stealing, (2) traffic accident (e.g. hit and run), (3) physical assault, (4) sexual comments/advances, and (5) public urination. The frequency was assessed on the basis of the observation during the previous 2 months (1 = once in 2 months, 2 = once per month, 3 = 2 or 3 times per month, 4 = once or more every week). The severity was assessed according to the degree of patient's awareness of his or her own antisocial behaviors (0 = full awareness, 1 = moderate awareness, 2 = mild awareness, 3 = no awareness). The NPI assesses BPSD on the basis of both frequency and severity; BPSD scores are obtained by multiplying the severity and the frequency scores. Therefore, the frequency and the severity scores were multiplied for each behavior, respectively, and then summed (maximum score = 60) to be used as covariate factor for SPM analysis in this study.

Table 1
Demographic variables of FTD patients

n	22	
Age (year)	62.9 (5.9)	Range: 52–74
Sex (M/F)	14/8	
Duration of illness (years)	4.1 (1.8)	Range: 2–9
Mini mental state examination (MMSE)	14.8 (7.7)	Range: 0–26
Hasegawa's dementia scale revised (HDS-R)	13.8 (7.1)	Range: 0–24
Raven's colored progressive matrices (RCPM)	22 (8.7)	Range: 5–33
Digit span		
Forward	4.6 (1.0)	Range: 3–7
Backward	2.3 (1.5)	Range: 0–4
Word learning (10 words)		
Immediate recall	1.6 (1.6)	Range: 0–4
Delayed recall (30 min)	1.1 (1.7)	Range: 0–4
Story recall (15 elements)		
Immediate recall	2.3 (2.4)	Range: 0–7.5
Delayed recall (30 min)	0.2 (0.6)	Range: 0–2
Ray-Osterrieth complex figure test		
Copy	27.5 (11.0)	Range: 5.5–36
Immediate recall	4.9 (6.9)	Range: 0–23
Delayed recall (30 min)	3.6 (7.1)	Range: 0–24
Stroop test		
Dot	58 (sec) (44.5)	Range: 19–132 (sec)
Word	120.7 (sec) (82.2)	Range: 27–165 (sec)
Word-dot	63.1 (sec) (47.4)	Range: 38–134 (sec)
Trail making		
Set A	335.6 (sec) (130.2)	Range: 255–621 (sec)

Note. Values are expressed as mean and (standard deviation). M = male, F = female, *n* = size, sec = second.

These antisocial behaviors were assessed independently by three geriatric psychiatrists (TA, SH, NK), who had not been given the information of the SPECT images. Whenever the scores were different among the psychiatrists, the mean score of the three psychiatrists was employed.

Brain SPECT procedure

Each subjects received an intravenous injection of 600 MBq of ^{99m}Tc-ECD while lying supine with eyes closed in a dimly lit, quiet

Table 2
Scores of antisocial behavior

Behavior	Scores of antisocial behavior	n
	Mean (SD; range)	
Stealing	6.38 (3.42; 0–12)	8/22
Traffic accident	3.46 (3.46; 0–12)	4/22
Physical assault	4.50 (4.34; 0–12)	8/22
Sexual comments/advances	7.67 (2.31; 0–9)	3/22
Public urination	3.67 (1.86; 0–6)	6/22
Total	9.67 (6.82; 0–25)	18/22

n = number of subjects who showed the behavior. n for total means of subjects who showed at least one of the behavior.

room. Ten minutes after injection, brain SPECT was performed using a triple-headed gamma camera (MULTISPECT 3; Siemens, Hoffman Estates, IL) equipped with high-resolution fanbeam collimators. For each scan, projection data were obtained in 128 × 128 matrix, and camera was rotated through 120° with 24 steps of 50 s per step. SPECT images were reconstructed using a Shepp and Logan Hanning filter at 0.7 cycles per centimeter. Attenuation correction was performed using Chang's method.

Image analysis

Voxel-based analysis of SPECT data was performed using Statistical Parametric Mapping 99 (SPM99) (Wellcome Department of Cognitive Neurology, London, U.K.) run on MATLAB (The MathWorks, Inc., Sherborn, MA). The images were spatially normalized to an original template for ^{99m}Tc-ECD using SPM99 (Ohnishi et al., 2000). Images were then smoothed with a gaussian kernel of 12 mm in full width half maximum (FWHM). The washout correction for ^{99m}Tc-ECD was not applied, because brain SPECT was started at 10 min after injection.

Statistical analysis of SPECT data

The processed images were analyzed using SPM99 as described by Ohnishi et al. (2000). The effect of global differences in CBF among scans was removed by proportional scaling with the gray matter threshold at 0.5. The subject and the covariate effects were estimated with a general linear model at each voxel. To test hypotheses about regional population effects, the estimates were compared using linear compounds or contrasts. The resulting sets of t values constituted statistical parametric maps (SPM$\{t\}$). The SPM$\{t\}$ were transformed to unit normal distribution (SPM$\{Z\}$) and thresholded at $P < 0.005$. To correct for the multiple non-independent comparisons that were inherent in this analysis, the resulting foci were characterized for their spatial extent. This characterization, regarding probability, is to assess whether the region of the observed number of voxels could have occurred by chance over the entire volume analyzed.

Correlation analysis was performed to study the relationship between rCBF changes and antisocial behavioral profiles. The correlations between the scores of antisocial behaviors and CBF, MMSE scores and CBF, and the duration of illness and CBF were respectively computed on a pixel-by-pixel basis by covariance analysis. Gender and age were treated as nuisance variables.

Statistical analysis of antisocial behavioral symptoms

Statistical data analysis of antisocial behavioral symptoms in FTD patients was performed using the R software (The R Foundation for Statistical Computing, Vienna, Austria).

Results

Antisocial behavioral symptoms in FTD patients

Eighteen of the 22 FTD patients had a history of antisocial behavior. The mean score of the antisocial behavior was 9.67 ± 6.82 (range, 0–25). The mean value of Cohen's κ coefficient of all the items for inter-rater was 0.82 (range, 0.67–0.91), which appears to be satisfactory. Table 2 shows the subscale score of the 5 antisocial behaviors of the patients.

Changes in rCBF in FTD patients

Decreases of rCBF in the FTD patients compared with the normal healthy volunteers were identified in the superior, the middle, and the inferior frontal gyrus. In addition, there were reductions of rCBF in the subcortical structures, particularly the caudate nuclei and the thalami (Fig. 1).

As a result of the correlation analysis, a positive correlation was observed between the scores of antisocial behavioral symptoms

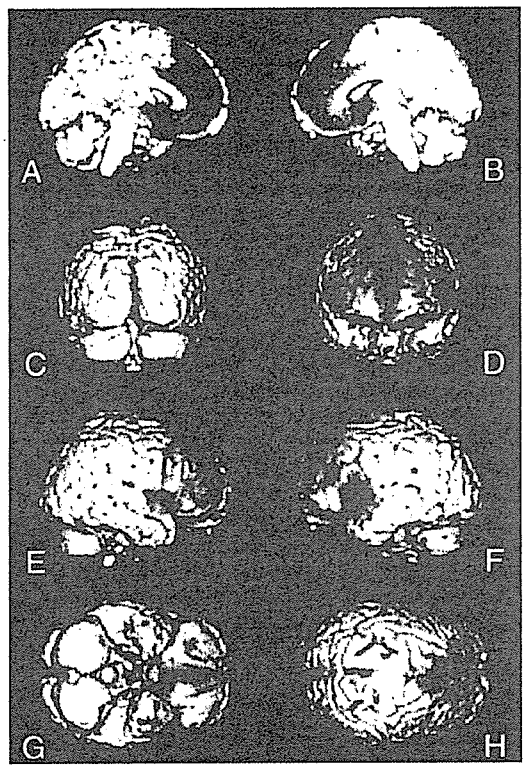

Fig. 1. Result of SPM analysis (normal healthy volunteers vs. FTD patients). The colored areas show the regions with lower perfusion in the FTD patients compared with the normal healthy volunteers ($P < 0.005$, uncorrected for multiple comparisons). View from medial right (A), medial left (B), posterior (C), anterior (D), right lateral (E), left lateral (F), inferior (G), and superior (H). Rt = right, Lt = left.

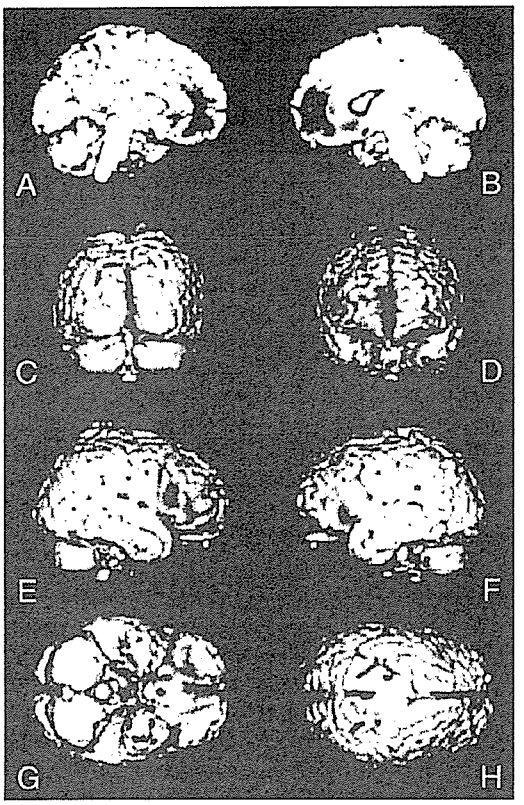

Fig. 2. Result of SPM analysis: the areas of regional cerebral blood flow that correlated with the score of antisocial behaviors in patients with FTD. Representation in stereotaxic space of cerebral regions that correlated positively with the score of antisocial behaviors ($P < 0.005$, uncorrected for multiple comparisons), displayed on 3D-surface anatomical template. View from medial right (A), medial left (B), posterior (C), anterior (D), right lateral (E), left lateral (F), inferior (G), and superior (H). Rt = right, Lt = left.

and the rCBF in partial areas of the orbitofrontal cortex (Fig. 2): the bilateral inferior frontal gyri (Broadmann area, BA 47), the left anterior cingulated gyrus (BA 32), the right caudate nucleus, and the left insula (BA 13). The results were similar even when the scores were independently analyzed for the severity scores and the frequency scores. We searched for a negative correlation between rCBF and the scores of antisocial behavioral symptoms, but no significant finding was found in any of the regions.

On the other hand, the MMSE scores positively correlated with rCBF in the bilateral posterior cingulate gyri (BA 31), the right parahippocampal gyrus (BA 30), and the right insula (BA 13) (Fig. 3). Furthermore, a correlation between the duration of illness and rCBF was observed in the right middle frontal gyrus (BA 47) and the bilateral inferior frontal gyri (BA 46, 47), as well as the left superior temporal gyrus (BA 22), the middle temporal gyrus (BA 21), and the parahippocampal gyrus (BA 27) (Fig. 4). The two analyses have resulted to have BA 47, which constitutes the orbitofrontal cortex, in common.

Discussion

FTD is the third most common neurodegenerative dementia syndrome after Alzheimer's disease and dementia with Lewy bodies. Although criteria for clinical diagnosis of FTD, such as the Lund and Manchester criteria and the more recent consensus criteria (Neary et al., 1998), have high sensitivities and specificities for diagnosing FTD (Lopez et al., 1999), clinicians frequently fail to recognize FTD or misdiagnose it as Alzheimer's disease, manic-depressive illness, schizophrenia, depression, hypochondriasis, obsessive–compulsive disorder, or sociopathy (Litvan et al., 1997; McKhann et al., 2001). The core diagnostic features of FTD are early loss of personal and social awareness, early loss of insight, early decline in social interpersonal conduct, impaired regulation of personal conduct, and emotional blunting. Thus, the most common and early symptom of FTD can be summarized as a decline in social interpersonal conduct (Neary et al., 1998).

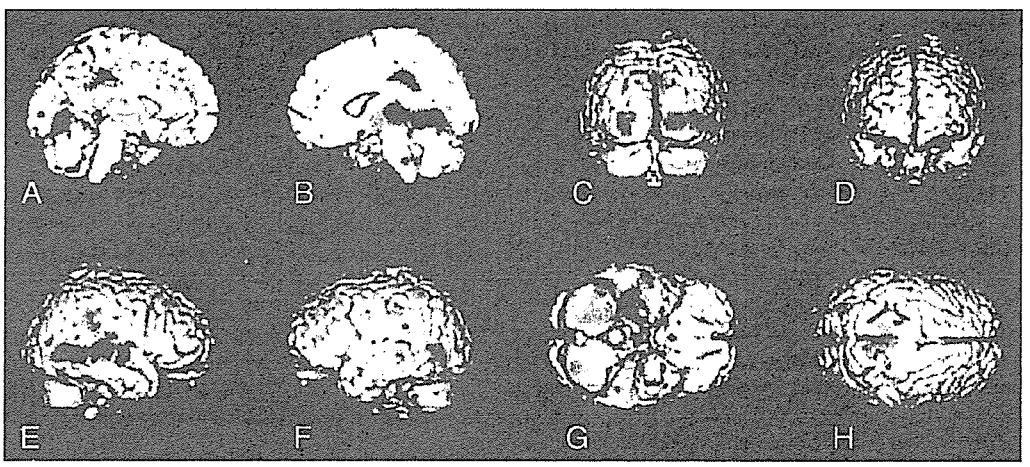

Fig. 3. Result of SPM analysis: the areas of regional cerebral blood flow that correlated with the score of MMSE in patients with FTD. Representation in stereotaxic space of cerebral regions that correlated positively with the score of MMSE ($P < 0.005$, uncorrected for multiple comparisons), displayed on 3D-surface anatomical template. View from medial right (A), medial left (B), posterior (C), anterior (D), right lateral (E), left lateral (F), inferior (G), and superior (H). Rt = right, Lt = left.

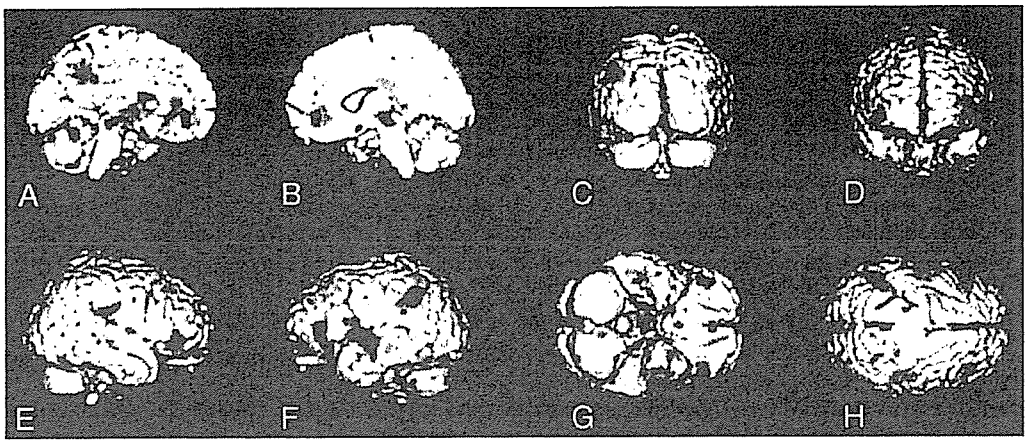

Fig. 4. Result of SPM analysis: the areas of regional cerebral blood flow that correlated with the duration of illness in patients with FTD. Representation in stereotaxic space of cerebral regions that correlated positively with the score of the duration of illness ($P < 0.005$, uncorrected for multiple comparisons), displayed on 3D-surface anatomical template. View from medial right (A), medial left (B), posterior (C), anterior (D), right lateral (E), left lateral (F), inferior (G), and superior (H). Rt = right, Lt = left.

Antisocial behavior, from Pick's case report (Pick, 1892), has been reported in association with FTD for decades (Gustafson, 1987; Lindau et al., 2000; Hokoishi et al., 2001; Hodges, 2001). They include stealing, traffic accident, physical assault, sexual comments/advances, public urination, and so on. In fact, 18 of 22 (82%) FTD patients of the present study showed such behaviors. This figure is similar with the results reported in the previous studies (Miller et al., 1997).

Although a variety of scales to rate the Behavioral and Psychological Symptoms of Dementia (BPSD) observed in patients with AD is reported, to our knowledge, no scale is available for the assessment of BPSD observed in FTD patients. Thus, we employed the assessment method of the Neuropsychiatric Inventory (NPI) (Cummings et al., 1994) for AD patients. The NPI assesses BPSD on the basis of both frequency and severity. The focused symptoms are derived from the report by Miller et al. on BPSD of FTD patients.

In the comparison between the FTD patients and the normal healthy volunteers, a significant reduction of rCBF in the widespread frontal lobes was observed in the former. No other region with significantly decreased rCBF was found. The results seem to be compatible with the neuropathological and functional changes of the disease and are consistent with the findings of previous FDG-PET studies (Ishii et al., 1998; Salmon et al., 2003; Grimmer et al., 2004). Although the diagnosis of the present study was not confirmed by postmortem examination, the result appears to support the validity of our diagnosis of FTD, the frontal variants of FTLD.

Regarding the frontal lobe function, it is well known that prefrontal cortex dysfunction is linked to social misconduct (Harlow, 1868; Eslinger, 1999; Bassarath, 2001; Brower and Price, 2001). Stuss and Benson (1986) have noted that orbitofrontal pathology would most frequently be associated with disinhibition, facetiousness, sexual and personal hedonism, and lack of concern for others. Moreover, a recent PET study evaluating patients with various frontal lobe pathologies (including FTD) (Sarazin et al., 1998) with ROI approach has revealed that the behavioral abnormalities are associated with metabolic decline of orbitofrontal cortex. Also, it is now well known that prefrontal cortex plays a major role in executive function and working memory (Lezak, 1983). Anterior cingulate gyrus and cortex are associated with sustained attention (Posner and Petersen, 1990). Although dysfunction of the orbitofrontal cortex plays a major role, failure of these cognitive functions may be functionally involved together and contribute to the development of the antisocial behaviors.

The highlight of our voxel-by-voxel SPECT study using the SPM technique is the finding that the decrement of orbitofrontal rCBF is associated with antisocial behaviors as well as the duration of illness in the patients with FTD. MMSE score, on the contrary, did not correlate with rCBF of the orbitofrontal cortex. A recent longitudinal study in FTD has shown that the metabolic activity in the orbitofrontal cortex decreases as the disease progresses (Grimmer et al., 2004). In this multicenter study, the conjunction analysis using SPM has demonstrated that the metabolic impairment of orbitofrontal cortex is affected in every FTD patients (Grimmer et al., 2004). Although this study did not examine the association between metabolic impairment of orbitofrontal cortex and antisocial behaviors, it may support the results of the present study to some extent. Taking these findings together, the association between antisocial behaviors and rCBF of orbitofrontal cortex in FTD may appear to be robust.

We must refer to several limitations of the present study. As described above, we did not pathologically confirm the clinical diagnosis. However, clinical criteria of FTD are reported to have high specificities (Rosen et al., 2002). SPM analysis for SPECT study also has limitations; it can be affected by partial volume effect (PVE). Matsuda et al. (2002) have established a PVE correction method for SPECT study and reported its utility. In this study, however, we did not correct the PVE. In future study, correlation analysis between antisocial behavior and rCBF using PVE correction is necessary. We also attempted to clarify the relationship between the duration of illness and rCBF, but since the onset of FTD is insidious and its progression is gradual, the duration of illness remained uncertain (Neary et al., 1998). Moreover, the number of the subjects was relatively small. Future studies should overcome these limitations.

In summary, the orbitofrontal dysfunction appears to play a major role in the emergence of antisocial behaviors in FTD patients.

References

Anne, T., Stephan, F., 1969. The Stroop test: selective attention to colours and words. Nature 222, 437–439.

Bassarath, L., 2001. Neuroimaging studies of antisocial behaviour. Can. J. Psychiatry 46, 728–732.

Brower, M.C., Price, B.H., 2001. Neuropsychiatry of frontal lobe dysfunction in violent and criminal behaviour: a critical review. J. Neurol. Neurosurg. Psychiatry 71, 720–726.

Charpentier, P., Lavenu, I., Defebvre, L., Duhamel, A., Lecouffe, P., Pasquier, F., Steinling, M., 2000. Alzheimer's disease and frontotemporal dementia are differentiated by discriminant analysis applied to (99m)Tc HmPAO SPECT data. J. Neurol. Neurosurg. Psychiatry 69, 661–663.

Cummings, J.L., Mega, M., Gray, K., Rosenberg-Thompson, S., Carusi, D.A., Gornbein, J., 1994. The neuropsychiatric inventory: comprehensive assessment of psychopathology in dementia. Neurology 44, 2308–2314.

Eslinger, P.J., 1999. Orbital frontal cortex: historical and contemporary views about its behavioral and physiological significance. An introduction to special topic papers: Part I. Neurocase 5, 225–229.

Folstein, M.F., Folstein, S.E., McHugh, P.R., 1975. Mini-mental state. A practical method for grading the cognitive state of patients for the clinician. J. Psychiatr. Res. 12, 189–198.

Frackowiack, R.S.J., Friston, K.J., Frith, C.D., Dolan, R.J., Mazziotta, J.C., 1997. Human Brain Function. Calif: Academic Press, San Diego.

Grimmer, T., Diehl, J., Drzezga, A., Forstl, H., Kurz, A., 2004. Region-specific decline of cerebral glucose metabolism in patients with frontotemporal dementia: a prospective 18F-FDG-PET study. Dement. Geriatr. Cogn. Disord. 18, 32–36.

Gustafson, L., 1987. Frontal lobe degeneration of non-Alzheimer type: II. Clinical picture and differential diagnosis. Arch. Gerontol. Geriatr. 6, 209–223.

Harlow, J., 1868. Recovery from passage of an iron bar through the head. Publications of the Massachusetts Medical Society 2, 329–346.

Hodges, J.R., 1993. Cognitive Assessment for Clinicians, 1st ed. Oxford Medical, Oxford, England, pp. 197–228.

Hodges, J.R., 2001. Frontotemporal dementia (Pick's disease): clinical features and assessment. Neurology 56, S6–S10.

Hokoishi, K., Ikeda, M., Maki, N., Nebu, A., Shigenobu, K., Fukuhara, R., Komori, K., Tanabe, H., 2001. Frontotemporal lobar degeneration: a study in Japan. Dement. Geriatr. Cogn. Disord. 12, 393–399.

Imabayashi, E., Matsuda, H., Asada, T., Ohnishi, T., Sakamoto, S., Nakano, S., Inoue, T., 2004. Superiority of 3-dimensional stereotactic surface projection analysis over visual inspection in discrimination of patients with very early Alzheimer's disease from controls using brain perfusion SPECT. J. Nucl. Med. 45, 1450–1457.

Imai, Y., Hasegawa, K., 1999. In: Burns, A., Lawlor, B., Craig, S. (Eds.), Assessment Scales In Old Age Psychiatry. Martin Dunitz, London, p. 71.

Ishii, K., Sakamoto, S., Sasaki, M., Kitagaki, H., Yamaji, S., Hashimoto, M., Imamura, T., Shimomura, T., Hirono, N., Mori, E., 1998. Cerebral glucose metabolism in patients with frontotemporal dementia. J. Nucl. Med. 39, 1875–1878.

Lezak, M.D., 1983. Neuropsychological Assessment, 2nd ed. Oxford UP, New York.

Lindau, M., Almkvist, O., Kushi, J., Boone, K., Johansson, S.E., Wahlund, L.O., Cummings, J.L., Miller, B.L., 2000. First symptoms-frontotemporal dementia versus Alzheimer's disease. Dement. Geriatr. Cogn. Disord. 11, 286–293.

Litvan, I., Agid, Y., Sastry, N., Jankovic, J., Wenning, G.K., Goetz, C.G., Verny, M., Brandel, J.P., Jellinger, K., Chaudhuri, K.R., McKee, A., Lai, E.C., Pearce, R.K., Bartko, J.J., 1997. What are the obstacles for an accurate clinical diagnosis of Pick's disease? A clinicopathologic study. Neurology 49, 62–69.

Lojkowska, W., Ryglewicz, D., Jedrzejczak, T., Sienkiewicz-Jarosz, H., Minc, S., Jakubowska, T., Kozlowicz-Gudzinska, I., 2002. SPECT as a diagnostic test in the investigation of dementia. J. Neurol. Sci. 15, 215–219.

Lopez, O.L., Litvan, I., Catt, K.E., Stowe, R., Klunk, W., Kaufer, D.I., Becker, J.T., DeKosky, S.T., 1999. Accuracy of four clinical diagnostic criteria for the diagnosis of neurodegenerative dementias. Neurology 53, 1292–1299.

Matsuda, H., Kanetaka, H., Ohnishi, T., Asada, T., Imabayashi, E., Nakano, S., Katoh, A., Tanaka, F., 2002. Brain SPET abnormalities in Alzheimer's disease before and after atrophy correction. Eur. J. Nucl. Med. Mol. Imaging 29 (11), 1502–1505.

McKhann, G.M., Albert, M.S., Grossman, M., Miller, B., Dickson, D., Trojanowski, J.Q., 2001. Work Group on Frontotemporal Dementia and Pick's Disease. Clinical and pathological diagnosis of frontotemporal dementia: report of the work group on frontotemporal dementia and pick's disease. Arch. Neurol. 58, 1803–1809.

Miller, B.L., Gearhart, R., 1999. Neuroimaging in the diagnosis of frontotemporal dementia. Dement. Geriatr. Cogn. Disord. 10, S71–S74.

Miller, B.L., Darby, A., Benson, D.F., Cummings, J.L., Miller, M.H., 1997. Aggressive, socially disruptive and antisocial behaviour associated with fronto-temporal dementia. Br. J. Psychiatry 170, 150–154.

Mychack, P., Kramer, J.H., Boone, K.B., Miller, B.L., 2001. The influence of right frontotemporal dysfunction on social behavior infrontotemporal dementia. Neurology 56, S11–S15.

Neary, D., Snowden, J.S., Gustafson, L., Passant, U., Stuss, D., Black, S., Freedman, M., Kertesz, A., Robert, P.H., Albert, M., Boone, K., Miller, B.L., Cummings, J., Benson, D.F., 1998. Frontotemporal lobar degeneration: a consensus on clinical diagnostic criteria. Neurology 51, 1546–1554.

Ohnishi, T., Matsuda, H., Hashimoto, T., Kunihiro, T., Nishikawa, M., Uema, T., 2000. Abnormal regional cerebral blood flow in childhood autism. Brain 123, 1838–1844.

Pick, A., 1892. Uber die Beziehungen der senilen Hirnatrophie zur Aphasie. Prager Medizinische Wochenschrift 17, 165–167.

Posner, M.I., Petersen, S.E., 1990. The attention system of the human brain. Ann. Rev. Neurosci. 13, 25–42.

Rosen, H.J., Hartikainen, K.M., Jagust, W., Kramer, J.H., Reed, B.R., Cummings, J.L., Boone, K., Ellis, W., Miller, C., Miller, B.L., 2002. Utility of clinical criteria in differentiating frontotemporal lobar degeneration (FTLD) from AD. Neurology 58, 1608–1615.

Salmon, E., Garraux, G., Delbeuck, X., Collette, F., Kalbe, E., Zuendorf, G., Perani, D., Fazio, F., Herholz, K., 2003. Predominant ventromedial frontopolar metabolic impairment in frontotemporal dementia. NeuroImage 20, 435–440.

Sarazin, M., Pillon, B., Giannakopoulos, P., Rancurel, G., Samson, Y., Dubois, B., 1998. Clinicometabolic dissociation of cognitive functions and social behavior in frontal lobe lesions. Neurology 51, 142–148.

Stuss, D.T., Benson, D.F., 1986. The Frontal Lobes. Raven Press, New York.

1. PDD（認知症を伴うParkinson病）とDLB（Lewy小体型認知症）の臨床と病理

東京都老人総合研究所高齢者ブレインバンク　村山繁雄
東京都老人医療センター剖検病理科　齊藤祐子

key words　α-synuclein, autonomic failure, substantia nigra, Lewy body, amygdala

略　号

PD: Parkinson disease（Parkinson病）
PDD: Parkinson disease with dementia（認知症を伴うParkinson病）
LB: Lewy body（Lewy小体）
DLB: dementia with Lewy bodies（Lewy小体型認知症）
AD: Alzheimer disease（Alzheimer病）
LBD: Lewy body disease（Lewy小体病）（Lewy body dementia: Lewy小体型認知症ではないことに注意）
SP: senile plaque（老人斑）
NFT: neurofibrillary tangle（神経原線維変化）
α-syn: α-synuclein
psyn: phosphorylated α-synuclein

要　旨

PDDとDLBは，McKeithらにより，認知症で発症するか，Parkinson病（PD）の発症と認知症の出現が1年以内ならDLBとする，いわゆる「1年ルール」で分類された．しかし，高齢者の場合PDの発症時に記憶障害を伴うことが一般的で，臨床的にこの区分は成立しない．神経病理学的にも，PDDは脳幹優位，DLBは辺縁系・新皮質優位の傾向をもち，Alzheimer病（AD）病変の合併はDLBに優位に多いが，両者の病理は大きく重なる．LB病変を，黒質・線条体系，辺縁・新皮質系，節前・節後自律神経系の三系統で評価し，AD病変と合わせ，臨床的Parkinson症状，認知障害，自律神経症状と，症例毎に対応させ検討していくことが，重要である．本来同一疾患であるPDDとDLBを別名でよぶことは混乱を招き，人口に膾炙しているPDに統合することが，今後の学問の発展上有用である．

動　向

本稿は，the 10th International Congress of Parkinsons's Disease and Movement Disorders (October 2006, Kyoto)[1]と，the 4th International Workshop on DLB and PDD (October 2006, Yokohama)[2]の成果を含め，特に後者での議論を中心に，できる限りup to dateの内容になるようにこころがけた．

両学会を通じ，PD (Parkinson disease: 認知症を伴わないParkinson病)/PDD (Parkinson disease with dementia: 認知症を伴うParkinson病)/DLB (dementia with Lewy body: Lewy小体型認知症）という三病名を連記する記述が頻回に用いられた．これらは，Kosakaにより，Lewy小体 (LB) 病 (LBD) と命名された群を指す．本来同一でよばれるべき疾患が，なぜ三つの病名でよばれなければならないか，またなぜLBD，ついでDLBという新しい病名がつくられなければな

らなかったかについては，歴史的経緯を述べる必要がある．

また，今回のPDD/DLB国際シンポジウムで，順天堂大学水野美邦，森　秀生両博士より，LBDは病理学的概念であり，臨床的な名称で人口に膾炙しているPDを包括的に用いることが，命名をめぐる混乱を終始させるのに有効であるという主張がなされた．実際，上掲二学会においても，いわゆるPD/PDD/DLBを臨床的に専門とする神経内科医・精神科医から，これら三者の病理学的鑑別について，多くの質問を受けた．しかし後述するように，純粋神経病理学的見地から，この三者を鑑別することは不可能である．私は，水野博士らの立場に全面的に賛成する立場より，このレビューを執筆する．

A. PDDとDLBの命名をめぐる歴史

PDは，James Parkinsonにより，安静時振戦，寡動，筋強剛，姿勢反射障害という臨床記載をもとに発表されたが，認知障害は伴わないと明記された．CharcotによりParkinsonの記載が再評価されたときも，運動障害が主症状で，認知障害はないとの疾患概念が，流布することとなった．

PD患者が認知障害をきたすことは，臨床面では観察されていたが，皮質下病変によるものでbradyphreniaとよぶべき思考過程の遅延で，時間をかければ達成できる点で，dementiaとは異なるという主張がされていた．また他の疾患の合併，治療薬剤の副作用をまず考えるべきであるという考えが主流であった．

一方，LBについては，1912年に，PDの迷走神経背側核とMeynert基底核において，Lewyがhematoxylin and eosin（HE）染色で特徴的封入体を初めて記載し，その後Tretiakoffが黒質で記載し，PDの中核病理であると指摘した．1953年Greenfiledは，Parkinson病においては，LBが脳幹に出現することが診断的意義を有することを教科書的に記載し，1960年代になり，PDの診断にはLBが必須であるという概念が定着した．

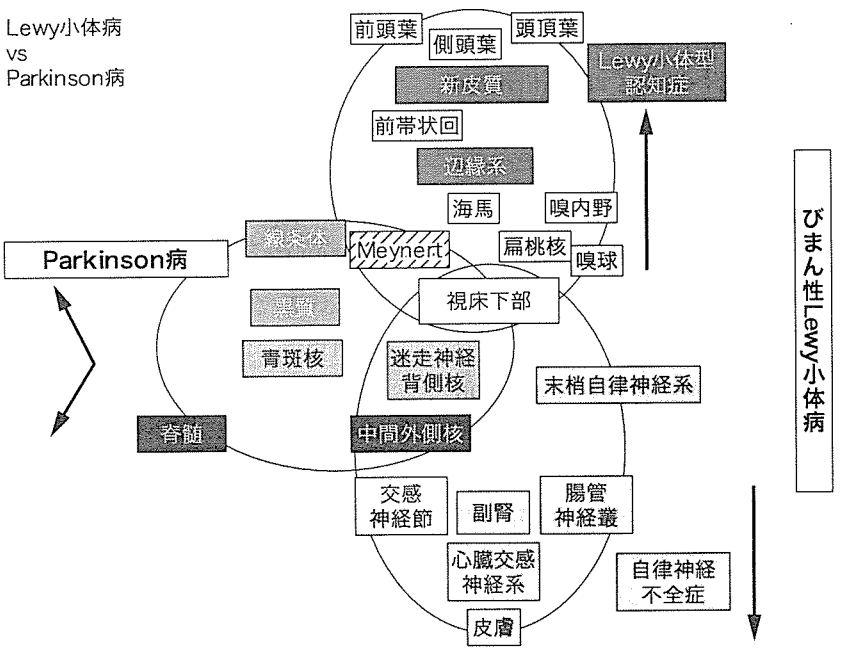

図1　Parkinson病（Lewy小体病）は全身疾患である

一方，Mayo ClinicのOkazakiらは，1961年，認知症で，幻視と筋強剛を呈する2症例で，皮質にLBを初めて記載したが，PDとの関係には言及しなかった．したがって，DLBの概念の成立には，1976年の，認知症，妄想，幻視，錐体外路症状を中核症状とする症例群に関する，小阪憲司博士の記述が大きく貢献している．小阪らは，病理学的検索より後方視的に臨床症状を抽出する手法をとり，LBの分布により，脳幹型，辺縁型，新皮質型に分類し，これらを総合的に，Lewy小体病（LBD）と命名した[3]．そして，辺縁型と新皮質型を含め，びまん性Lewy小体病（diffuse Lewy body disease: DLBD）[4]と命名し，認知症の責任病理となりうること，脳幹型が臨床的にParkinson病とほぼ一致するが，臨床と病理は完全には一致しないことを指摘した．

しかし，皮質型LBを，HE染色だけで見分けることは，欧米の神経病理学者には困難であったことより，この疾患概念はなかなか普及しなかった．1984年になり，抗ubiquitin抗体免疫染色で，LBが高感度に認識されるという，Kuzuharaら[5]の業績により，はじめて皮質型LBが容易に検出可能となった．これを受けて，第1回国際シンポジウムが開催され，DLBコンセンサスガイドラインが1996年に提出された[6]．

この段階で，Parkinson病関連認知症ともいうべきこの疾患群には，DLBDを含め，PD変化を伴うAlzheimer病（AD），偶発性Lewy小体を伴うAD，Lewy body variant of AD，senile dementia of Lewy body type等の名称が乱立していた．その解決として，McKeithはDLBの名称を新たに作り，その定義として，認知症がありLewy小体があればそうよぶという，包括概念を呈示した．その結果，ADとの線引きの問題は将来の検討課題となった．

臨床的診断基準として，中核症状，支持徴候，示唆徴候が定められ，症状の変動が，中核症状に含められた．

さらにこのガイドラインで，小阪らのLB進展分類に従い，HE染色あるいは抗ubiquitin抗体免疫染色により，辺縁系と新皮質のLewy小体の数に基づいてLewy scoreを算出し，脳幹・辺縁系・新皮質型に分類する病理診断基準が呈示された．しかし，ubiquitinは，元々ADの神経原線維変化（neurofibrillary tangle: NFT）より分離されたもので，LBを描出するだけでなく，NFTや老人斑（senile plaque: SP）を強く認識するため，HE染色での確認が本来必須である点が，ADとの鑑別に問題を残した．

さらに，このガイドラインで，DLBとPDDを分けるにあたり，認知症で始まるか，Parkinson症状の初発と認知症の初発が1年以内であればDLBとする，いわゆる「1年ルール」が採用された．なぜDLBとPDDを分類しなければならなかったかは，前者が物忘れ外来（memory clinic）を拠点とするのに対し，後者は運動障害クリニック（movement disorder clinic）を拠点とするため，住み分けをめざしたもので，科学的根拠に基づくものでないことは，第4回DLB/PDDシンポジウムでも，McKeithは明言している．実際，PDで経過し，認知症を発症したらDLBと診断名が変わることは，日常診療上も混乱を招くという主張は，理解可能である．

このガイドラインの功績は，PDD/DLBが，明らかな病理学的背景をもつ疾患で，ADとは異なることが確立されたことである．しかし，欧米の臨床では汎用されているCERAD（consortium to establish registry for Alzheimer disease）の診断基準では，ADの1/3にはLBが出現すると，論評なく単に記述されている[7]．Lewy body variant of Alzheimer diseaseの提唱者のPittsburgh大学のHamiltonらは，ADの60%にはLBが合併するという発表を繰り返している．Washinton大学のMorrisらは，SPが一定量ある認知症をす

べてADと診断する結果，DLBでSPを伴うものはすべてADと診断される．このように，ADとPDD/DLBの鑑別が，重要な課題として残る結果となった．

その後，遺伝性PDの責任遺伝子としてα-synuclein（α-syn）が同定され[8]，LBの主成分であることが，生化学的，免疫組織学的に明らかにされた[9]．抗α-syn抗体を用いた免疫組織化学により，LBのみならず，その前駆体であるpale body，Lewy neuritesが特異度・感度ともに高く検出されるようになった[10]．またα-synは129番位のSerineでリン酸化を受け不溶化することが明らかとなり[11]，リン酸化部位に対する抗体を用いることで，より高い特異度・感度で，LBを染色できるようになった[12]．その結果，PD/PDD/DLBの重なりはより明瞭になり，純粋病理学的観点から三者の分類は困難であることが，ますます明らかとなってきた．

また，α-synも，LBとの関連が解明される前に，SPの中で，amyloid β蛋白（Aβ）以外のcomponent，non amyloid component（NAC）として同定されたものと同一である．実際LBを伴う症例では，老人斑周囲の変性突起が，抗α-syn抗体免疫染色で陽性に染色される．それだけでなく，presenelin 1変異の家族性ADでは，扁桃核に高率に，抗α-syn抗体免疫染色陽性のLBが出現することが明らかとなった[13]．またLB病変と，SP，NFTはしばしば共存し，これらはいずれもが，出現の拡がりに関して正の相関をとることが明らかとなってきた[14]．つまり，PD病変とAD病変の密接な関係が，ますます明らかとなってきた．

さらに，若年者と高齢者のPD病変の比較より，前者では黒質・線条体系に病変が比較的限局するのに対し，後者では，初期より末梢自律神経系，辺縁系・新皮質にLBが出現する点で，病変が広範囲に及びやすいこと，それが高齢になるとL-dopaによる治療反応性が低下する現象を規定する根拠となっていることが，我々の検討より明らかとなってきた．

前記二学会においては，Hallidayにより，PD/PDD/DLBの表現型を規定するのは，認知症までの経過の長さと合併病変であること，Dudaにより，併発するAD病変の程度差であることが発表されたが，これは，我々の経験とも一致する．

2004年Braakらは，小阪らの進展分類に従うかたちで，認知症を伴わない高齢者とParkinson病例，すなわちDLBを除外した一般高齢者群におけるLB進展分類を，抗α-syn抗体を用いた免疫組織化学をもとに発表した[15]．それによれば，LBは迷走神経背側核より脳幹を上行し，辺縁系・新皮質に及ぶ．臨床的に，脳幹ステージ後期・辺縁型ステージがPD，辺縁系ステージ後期・新皮質ステージがPDDにほぼ相関すると記載した．しかしこのステージ分類は，認知症例を除外しているので，高齢者への適用は事実上不可能である．

臨床診断基準の見直しと，AD病変との線引きのため，1995年，第3回Consensus Guidelineで，改訂病理診断基準が定められた[16]．今回は，Braakステージ分類に従い，抗α-syn抗体免疫染色を用いた半定量評価が採用され，脳幹とMeynert基底核が評価箇所に加えられた．また，併存するAD病変の強さに基づき，LB病変が認知症に関与している可能性を，low，intermediate，high likelihoodの三段階で評価する方法が採用された．

この改訂ガイドラインの問題点について，第4回シンポジウムでの議論を中心に，個別に論究する．

B. PD/PDD/DLBと，非αシヌクレイノパチー家族性PD

LBDは，小阪らのオリジナルな定義では，PDとDLBを包括する概念である．それでは，LBDを水

野らの主張のように，PDと総称した場合問題となるのが，LBを伴わない遺伝性PDの存在である．

ADと家族性ADが，SPとNFT，すなわちAβとタウ蛋白（以下τ）の沈着を前提とするのとは異なり，PDは，LBの出現，すなわちα-syn沈着を必須としない．PDの定義は，臨床的にParkinson病の四徴である，安静時振戦，寡動，筋固縮，姿勢反射障害のうち，報告者の判断基準により二つないし三つ以上を呈し，抗Parkinson病薬に反応し，病理学的に黒質変性を示し，他の変性疾患が除外できることである．孤発性PDの場合はLBの存在が要求されるが，家族性の場合には，これを必須としない．したがって，家族性PDで常にLewy小体を伴うのは，α-syn遺伝子異常を伴う群にとどまる．

現在遺伝性Parkinson病は，遺伝子座の順に命名する作業が進行しているが，Lewy小体が確実に出現するPDは，Park 1, 4のみである．たとえばparkin遺伝子変異であるPark 2は，本邦で病態の臨床・画像・病理・分子病理のすべてが解明されたが，常染色体劣性遺伝で，Lewy小体の記載はほとんどなく[17]，純粋黒質変性の所見をとる．また，LRRK2遺伝子変異によるPark 8は，遺伝子座は本邦相模原家系で最初に決定されたが，剖検例において黒質変性は共通するが，同一家系内においても，LBを伴う少数群と，伴わず純粋黒質変性を示す群に加え，進行性核上性麻痺様のタウオパチーを呈する例が報告されている．

ただ，これらα-syn沈着を伴わない家族性PDは頻度的にはきわめて低いわけで，これを根拠に，PD/PDD/DLBという，混乱を招く用語を用いることを正当化できるかどうかは，さらに議論の必要があろう．

C. PD/PDD/DLBのゲノム神経病理

Park 1が同定されたあと，Park 4がα-syn遺伝子の三重複であることが明らかとなり[18]，この表現型はDLBであった．その後家族性PDの解析より，α-syn遺伝子の重複の症例が発見され[19]，この表現型はPDで，高齢になるとPDDになる例もあることが報告された[20]．さらに，ゲノムワイドスクリーニングにより，PDの危険因子として，α-syn遺伝子が検出され，PD発症危険因子となる多型は，脳におけるmessage発現が増加していることが明らかとなった[21]．これらの結果は，α-synの発現レベルと加齢の両方が，PD/PDD/DLBの発症年齢と症状に影響を与えていることが，明らかになりつつある．今後ゲノム面での研究の重要性を示唆している

D. PD/PDD/DLBの末梢自律神経病理

LBを伴うprogressive autonomic failure (LBAF)の病理学的研究から，LBは末梢自律神経系に出現し責任病理を形成し，進行するとPDないしDLBの病理を合併することが示された[22]．すなわち，Lewy小体病（Lewy body disease）は，中枢神経系のみならず，末梢自律神経系を侵す，全身疾患である（図1）．

本邦において，Lewy小体の出現を，最も特異度・感度ともに高いかたちで検出する方法として，^{123}I-MIBG（metaiodobenzylguanidine）心筋シンチグラフィーが汎用されている．もともと，心臓交感神経機能を評価する目的で開発され，心筋梗塞後の心不全の予後判定に，保険適用となっている．1990年代に，多系統萎縮症（multiple system atrophy: MSA）で低下することが示されたのが最初であるが，織茂らの剖検例を用いた検討により，脚光を浴びる結果となった[23]．当施設での検討でも，^{123}I-MIBG心筋シンチグラフィーで低下を認めた剖検例はすべて，左室前壁無髄線維の減少と抗tyrosin hydroxylase (TH) 抗体免疫染色性の低下に加え，抗phospohrylated α-synuclein

抗体陽性軸索を認めている[24].

第4回DLB/PDD国際シンポジウムにおいて，MIBG心筋シンチを含め，自律神経徴候を，PDD/DLBの示唆徴候でなく，支持徴候に昇格すべきであるとする本邦からの主張は継続審議となった．欧米の専門家からの慎重意見として，高齢者の場合，心筋障害を伴う可能性が高く，それをどう除外するかを示すべきとの主張がされた．これには心電図・心エコーを含む，慎重な検討が必要となろう．糖尿病等，他の末梢自律神経障害をきたす疾患の合併も，留意事項となろう．薬剤について，MAOB阻害薬は，結果に影響することがわかっているが，他の薬剤の影響についても検討を続ける必要がある．ADに関しては，臨床検討であるが，1/3で低下するとの報告があり[25]，剖検による確認が必要である．交感神経節前線維しか障害されないMSA等でも，進行期にはMIBG心筋シンチの取り込みは低下する点も，注意事項である．

E. PD/PDD/DLBの画像診断

今回のDLB/PDD国際シンポジウムにおける，MIBG心筋シンチをめぐる議論で，本邦研究者が，MIBG心筋シンチ診断を，他のモダリティーで確認していない点が指摘された．

ヨーロッパ連合では，dopamine transporter（βCIT）SPECTがPDに関する特異度・感度80％で診断手技として採用されたが，日本では使用不能である．dopamine合成能（[^{11}C]CFT, [^{18}F]F-DOPA），結合能（[^{11}C]$_n$-methyl spiperone, [^{11}C]raclopride）のPETは，特異度・感度ともに高いが，施行施設がきわめて限られており研究の範囲を出ない．

Minoshimaらは，FDG-PETによる後頭葉代謝低下が，特異度・感度ともに80%以上であるので[26]，支持徴候として採用するよう提言したが，継続審議となった．本邦では保険適応外だが，米国ではMedicaidレベルで採用されている．脳血流SPECTによる後頭葉血流低下は，特異度・感度がPETより低下するが，重要な診断根拠となる．

除外診断として有用なのが，中脳被蓋と橋底部の面積ならびに比をとる方法で[27]ある．当施設で剖検例での確認を遂行中であるが，Parkinson病群と，進行性核上性麻痺・皮質基底核変性症群，多系統萎縮症群は，特異度・感度90%以上で鑑別が可能である．

F. PD/PDD/DLBとAD病変との関係

PDは，Meynert基底核をはじめとする前脳基底核コリン作動性神経システムの病変が早期から存在することは，剖検例の検討から昔よりよく知られている．高齢者のPDを神経心理学的に検索すると，記憶障害型軽度認知障害（amnestic MCI）[28]の定義を満たす頻度が高く，PDD/DLBの準備状態であると考えられる．さらに，他のPD/PDD/DLBの前駆症状として，REM睡眠関連行動以上[29]，嗅覚低下の感度・特異度の問題が取り上げられ，さらに検討が必要との結論となった．

DLBに関しては，特にattentionの低下が，ADとの鑑別上重要であることがいくつかの施設より発表された．それに対し，精神症状の変動については，より客観的なパラメータを設ける必要性が指摘された．

DLBは，日本においては小阪らにより病理学的に，純粋型，通常型，AD型，脳型に分けられている．純粋型は，老年性変化がほとんどない群，通常型は老年性変化を伴う群，AD型はADの診断基準を満たすレベルのAD変化を伴う群，脳型は，新皮質中心にLBを伴う群である．脳型は特殊であり，高齢者ブレインバンク中には一例もない．一方，欧米において，DLBは純粋型しか一

般にはよばれない傾向が強く，通常型，AD型は，ADに含まれる傾向が強い．これは，同じ病気が国内外で別の名前でよばれていることを意味し，PD/PDD/DLBとADの臨床症状に関する議論をさらに複雑にしている．

AD病変，特にSPの存在は，皮質へのα-syn沈着の進展に大きな影響を与えていることは，我々の高齢者ブレインバンクを用いた検討からも明らかである[14]．すなわち，大脳皮質に老人斑が多いほど，α-syn沈着も強い[30]．

一方，小阪らの純粋型と通常型は，老人斑の沈着の程度でわけられており，髄液バイオマーカーのうちAβ値が両者の鑑別に有効である臨床観察[31]を，我々は剖検例で確認している．さらに最近Pittsburgh Compound B (PIB) によるAβPETで，臨床的鑑別がより確実になりつつある．

前記二つの国際会議で，線条体のα-syn沈着[32]とAβ沈着が，PDDよりDLBで著明であることが述べられ，認知症への関与が強調された．ただ，線条体へのAβ沈着は，PIBにおいて初期より高度集積が認められることより最近強調されてきたが，皮質のAβ沈着と相関し，Aβ誘導α-syn沈着が，新皮質だけでなく線条体でも観察されると解釈できる．

むすび

PDD/DLBは，PD/PDD/DLBと表記される同一疾患における，発症年齢の違いとAD病変の合併の程度に規定された，発現型の違いである．これらをLBDと統括するより，より人口に膾炙したPDと呼称する方が，より有用であるという水野美邦博士らの意見に賛成を表明することで，むすびにかえたい．

文献

1) Mizuno Y, editor. Abstracts of the 10th International Congress of Parkinson's disease and Movement Disorders. Kyoto: Wiley- Liss; 2006.
2) Kosaka K, editor. Abstracts of the fourth International Workshop on Dementia with Lewy bodies and Parkinson disease with dementia. Yokohama; 2006.
3) 小阪憲司, 松下正明, 小柳新策, 他. Lewy小体病の臨床病理学的研究. 精神神経学雑誌. 1980; 82(5): 292-311.
4) Kosaka K, Yoshimura M, Ikeda K, et al. Diffuse type of Lewy body disease: progressive dementia with abundant cortical Lewy bodies and senile changes of varying degree--a new disease ? Clin Neuropathol. 1984; 3(5): 185-92.
5) Kuzuhara S, Mori H, Izumiyama N, et al. Lewy bodies are ubiquitinated. A light and electron microscopic immunocytochemical study. Acta Neuropathol (Berl). 1988; 75(4): 345-53.
6) McKeith IG, Galasko D, Kosaka K, et al. Consensus guidelines for the clinical and pathologic diagnosis of dementia with Lewy bodies (DLB): report of the consortium on DLB international workshop. Neurology. 1996; 47(5): 1113-24.
7) Mirra SS, Heyman A, McKeel D, et al. The Consortium to Establish a Registry for Alzheimer's Disease (CERAD). Part II. Standardization of the neuropathologic assessment of Alzheimer's disease. Neurology. 1991; 41(4): 479-86.
8) Polymeropoulos MH, Lavedan C, Leroy E, et al. Mutation in the alpha-synuclein gene identified in families with Parkinson's disease. Science. 1997; 276(5321): 2045-7.
9) Spillantini MG, Schmidt ML, Lee VM, et al. Alpha-synuclein in Lewy bodies. Nature. 1997; 388(6645): 839-40.
10) Baba M, Nakajo S, Tu PH, et al. Aggregation of alpha-synuclein in Lewy bodies of sporadic Parkinson's disease and dementia with Lewy bodies. Am J Pathol. 1998; 152(4): 879-84.
11) Fujiwara H, Hasegawa M, Dohmae N, et al. alpha-Synuclein is phosphorylated in synucleinopathy lesions. Nat Cell Biol. 2002; 4(2): 160-4.
12) Saito Y, Kawashima A, Ruberu NN, et al. Accumulation of phosphorylated alpha-synuclein in aging human brain. J Neuropathol Exp Neurol. 2003; 62(6): 644-54.
13) Lippa CF, Fujiwara H, Mann DM, et al. Lewy bodies contain altered alpha-synuclein in brains